Journal of Nano- and Electronic Physics
Vol. **18** No 1, 02006(6pp) (2026)

Журнал нано- та електронної фізики
Том **18** № 1, 02006(6cc) (2026)

REGULAR ARTICLE

Self–Heating Effect in GaN Diode with Graded InGaN Mesa

V.O. Zozulia* ✉, O.V. Botsula, L.V. Pavlova, O.V. Degovtsov

V.N. Karazin Kharkiv National University, 4, Svoboda Sq., 61077 Kharkiv, Ukraine

(Received 20 December 2025; revised manuscript received 15 April 2026; published online 29 April 2026)

The multifunctional active elements which are an n-type GaN-based channel on the sapphire substrate with InGaN flat-topped structure (a mesa) on top of channel surface are presented in the article. A mesa is a graded layer with a molar Ga fraction varying from 0 at the cathode contact to 1 in the channel, forming complex diode cathode. The structures with two types of doping profiles (uniform doping and doping profile with a low concentration region) with carrier concentrations of $6 \cdot 10^{22}$ and 10^{23} m^{-3} in the channel, and lengths of 1.28 μm, 2.56 μm, and 5.12 μm are considered. The diode simulation has been carried out by using the Ensemble Monte Carlo Technique taking into account impact ionization and self-heating effect. The model applied to analyze temperature distribution in diode is provided. The temperature effect on the diode characteristics with direct current, as well as, the spectral (noise) characteristics of diode in conditions of a strong electric field are investigated.

It has been found that possible modes of operation are determined by the impact ionization effect, as well as the temperature and its redistribution in diode channel by self-heating effect. Impact ionization occurring in a strong electric field leads to self-oscillation in a diode. In the diode with the length of 5.12 μm it causes non-uniform heating due to the emergence of a moving strong field domains. Self-heating in short diodes leads to increasing threshold voltage which corresponds to current growing due to impact ionization. It has been shown that it is possible to stabilize strong electric fields near the cathode using a doping profile with a low concentration area, which contributes to a more uniform distribution of the electric field and temperature. The considered diodes can be used as a source of high frequency noise, a Gunn-like oscillator or a source of the high order harmonics in frequency multipliers.

Keywords: Graded layer, GaN, InGaN, Diode, Temperature, Electric field strength, Self-heating effect, Impact ionization, Noise, Oscillation, Spectral density.

DOI: 10.21272/jnep.18(2).02006 PACS numbers: 85.30.Fg, 73.40.Kp, 73.40. – c

1. INTRODUCTION

The use of nitride compounds (GaN, AlN, InN, BN, and their alloys) in semiconductor electronic devices is determined by their exceptional physical and electrical properties. These materials possess a wide band gap, high breakdown electric field strength, high melting temperature and heat capacity [1, 2].

Moreover, their ability to form a high-density two-dimensional electron gas (2DEG) with high electron mobility, which enables the development of high-frequency and high-power electronic devices should be noted as well [3, 4].

However, high current density flowing through nitride-based devices, strong electric fields, and large optical phonon energies can lead to a significant temperature rise within the device. Self-heating effects become substantial in submicron devices, where heat dissipation is limited [5]. These effects are further enhanced in case of ternary and quaternary nitride compounds and heterojunctions [6, 7].

The temperature increase in ternary and quaternary nitride-based solid solutions is a result of their lower thermal conductivity compared to binary compounds [7]. In compounds with a high indium content the band gap becomes narrower (0.7 eV in InN) and an increase in temperature may lead to a higher carrier concentration as a result of thermal generation and impact ionization. In heterojunctions heat transfer is further complicated by interface effects occurring at the boundary between two different materials [8]. Thus, power density of some parts of a device with low power dissipation can be order of magnitude higher than the average power density of the whole device.

The high melting temperature of nitrides, however, does not guarantee their stability under operating conditions. Stresses caused by different rates of thermal expansion of materials that form a device can lead to device failure [9]. This is primarily an issue for contact regions, which are formed at significantly lower temperatures. In fact, thermal degradation of contacts is the main factor determining the operating temperature of nitride-based devices.

All the abovementioned effects are present in ultrahigh-frequency devices, since their dimensions are quite small and heat dissipation is limited. The formation of strong electric field regions and impact ionization processes often play a dominant role in their operation [10]. Therefore, accounting for self-heating effects becomes

* Correspondence e-mail: v.zozulia@karazin.ua

© 2026 The Author(s). Journal of Nano- and Electronic Physics published by Sumy State University. This article is distributed under the terms and conditions of the Creative Commons Attribution (CC BY) license.

Cite this article as: V.O. Zozulia et al., *J. Nano- Electron. Phys.* 18 No 2, 02006 (2026) https://doi.org/10.21272/jnep.18(2).02006

essential for determining their characteristics and operating modes.

In order to investigate and understand mechanisms responsible for the temperature-induced degradation of nitride-based diode characteristics modeling and simulation results of the self-heating effect in a planar diode under strong electric fields and impact ionization, as well as a possible approach to improving the diode performance are presented in the paper.

2. STRUCTURE AND SIMULATION

A microwave high-frequency device consisting of a semiconductor structure which contains heterogeneous regions formed from different materials and operating in a mode close to electrical breakdown has been selected for analysis of their thermal parameters. A cross section of the planar diode is shown in Fig. 1.

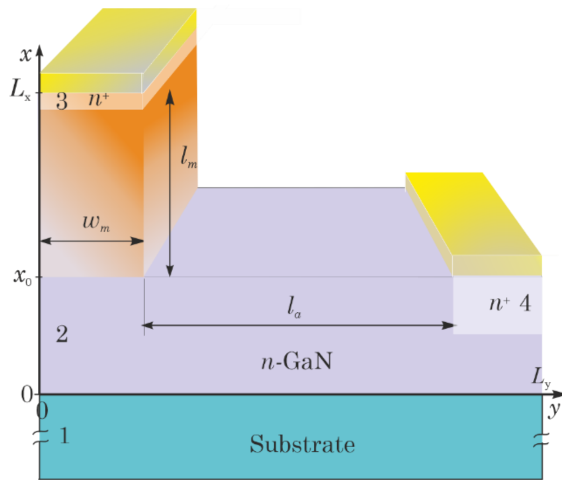

Fig. 1 – The planar GaN diode structure with a InGaN-based mesa

The diode contains a GaN channel formed on a sapphire substrate (1) and a complex cathode contact representing a mesa structure based on a graded InGaN layer (2). The active region of the diode is a part of n-type channel located between the n^- region and the n^+ contact region of the anode.

The doping profile and composition distribution in diode is shown in Fig. 2.

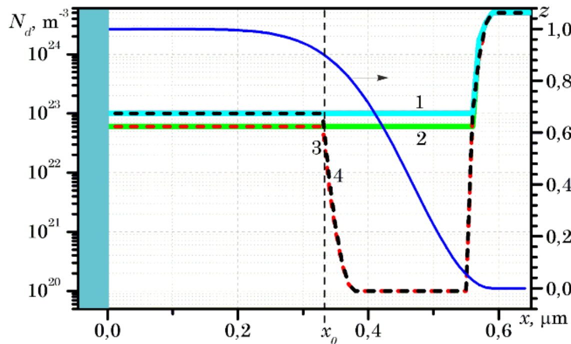

Fig. 2 – Composition distribution $z(x)$, and types of doping profiles: 1, 2 are the type 1; 3, 4 are the type 2; 1, 4 are 10^{23} m^{-3}; 2, 3 are $6 \cdot 10^{22}$ m^{-3}

Two types of doping profiles have been considered. The first is uniform doping (type 1), 1, 2 in Fig. 2. The second one is doping profile with low concentration region (type 2), 3, 4 in Fig. 2. Carrier concentration in a channel is $6 \cdot 10^{22}$ and 10^{23} m^{-3} respectively. Diodes of the lengths of 1.28 µm, 2.56 µm, and 5.12 µm have been examined.

Due to presence of the n^--region, a high electric field region or the cathode static domain (CSD) is formed near the cathode. The doping concentrations in the low doped regions are chosen to ensure stabilization of the CSD. An active diode element with a CSD can be used both for generation of electromagnetic oscillations at frequencies above 100 GHz and, under certain conditions, for generation of microwave noise. In conditions of strong electric field the probability of impact ionization becomes significant.

When the diode is used as a source of microwave noise, impact ionization is one of the key factors. Therefore, the self-heating effect of the diode becomes substantial, and thermal analysis of the device is an essential procedure.

The two-dimensional model of a diode corresponding to the x-y coordinate plane in Fig. 1. is analyzed. The composition distribution in the $In_zGa_{1-z}N$ compound is described by the relation $z(x) = 1 - \exp(-(x - x_0)^2 / 2\sigma^2)$, where x_0 denotes the point corresponding to the interface separating the cathode mesa structure and the diode channel, and is the parameter defining the width of the graded-composition layer. The value $z = 1$ corresponds to InN, while $z = 0$ corresponds to GaN. The n^+-regions represent heavily doped contact areas, and the n^--region is characterized by a low dopant concentration.

The diode model assumes that all metal semiconductor contacts are ohmic. To ensure this, the dopant concentration in the n^+-regions is considered to be $5 \cdot 10^{24}$ m^{-3}, which in practice provides contact behavior close to that of an ohmic contact.

To determine influence of the self-heating effect on the device performance, the Ensemble Monte Carlo method has been employed self-consistently with the solution of the Poisson and heat equations. The band structure model of $In_zGa_{1-z}N$ included three lower conduction band valleys (Γ, Γ_1, and M–L valleys). For the conduction band valleys, the deviation of the dispersion relation from the parabolic law has been taken into account.

It is assumed that the maximum bias voltage of the diode corresponds to the onset of impact ionization, which takes place in the graded cathode region. In these conditions, the anisotropy of the valence band can be neglected, and it can be described only by the heavy-hole subband that defines the threshold voltage of impact ionization.

Scattering of charge carriers by polar optical phonons, deformation potentials of optical and acoustic phonons, piezoelectric scattering, and scattering by ionized impurities have been considered in this research. For electrons, intervalley scattering has been taken into account as well. In the graded-composition region, scattering due to the alloy potential has been additionally included.

In the calculation region with dimensions $L_x \times L_y$, a uniform grid is introduced:

$$\Omega_h = \left\{ (x_i, y_j) \middle| x_i = ih_x, y_j = jh_y, 0 \le i \le N_x + 1, 0 \le j \le N_y + 1 \right\} \quad (1)$$

where $h_x = L_x/N_x$ is the step along the x-axis; $h_y = L_y/N_y$ is the step along the y-axis; and N_x, N_y are the numbers of discretization layers.

To determine the charge density $\rho(x_p, y_p)$ at the grid nodes and to reproduce the force acting on the particle at point (x, y) the charge of the particle $q_L = Q_L/N$ has been redistributed among the grid nodes x_p, y_p of the grid according to its form factor $W(x - x_p, y - y_p)$ using the CIC method [11]. The distribution of electric potential has been found from Poisson's equation, taking into account the dependence of the dielectric permittivity $\varepsilon(z)$ on the composition in the graded $In_zGa_{1-z}N$ layer in accordance with [12].

The potentials φ_C at the cathode contact and the potential φ_A at the anode contact have been set to fixed values: $\varphi_C = 0$ and $\varphi_A = \Delta\varphi + V$, where $\Delta\varphi$ is the difference in contact potentials due to the conduction band discontinuity and the difference in chemical potentials of the cathode and anode materials. Neumann boundary conditions have been applied at the other device boundaries.

To determine the electric potential distribution $\varphi(x, y)$ in the diode, equation (1) has been discretized on the grid Ω_h using a five-point stencil. To find the potential distribution at the nodes of Ω_h the full multigrid method (FMG) [13], previously employed for modeling planar structures with graded-composition layers having similar geometry, has been used [14].

In the graded layer of the cathode quasi-electric fields determined by the coordinate dependence of the band structure of the material's (the position of the conduction band energy minima, the effective mass, and the nonparabolicity coefficient), act on the charge carriers as well. Forces acting on electrons and holes F_n and F_p, are the sum of the electric field forces and the quasi-electric field forces:

$$F_n = F_{En} - e\nabla\left(\Delta E_C(x)\right) + \frac{E_e}{m_e^*} \frac{\nabla m_e^* + E_e \nabla\left(m_e^* \alpha\right)}{1 + 2\alpha E_e}, \quad (2)$$

$$F_p = F_{Ep} + e\nabla\left(\Delta E_V(x)\right) + \frac{E_p}{m_p^*} \nabla m_p^*, \quad (3)$$

where $\Delta E_C(x)$ and $\Delta E_V(x)$ represent the coordinate-dependent changes in potential energy caused by the variation in material composition. The magnitude of the electric forces F_{En} and F_{Ep} has been determined considering the particle form factor by using the CIC scheme according to the electrostatic potential values at the grid nodes. The magnitude of the quasi-electric force has been determined locally at the particle's position. The details of the mathematical model and material parameters correspond to [15-17].

The object under analysis is considered to be a limiting case from the perspective of the methods currently used for determining thermal regimes of nitride-based devices. On the one hand, the total device length is comparable to ten mean free paths of the phonons. That allows us to use the classical heat conduction equation. On the other hand, the presence of interfaces between the contacts and the active region of the diode, as well as the boundaries between the active region and the substrate, requires consideration of the thermal properties of interfaces, which can significantly influence heat transfer and self-heating effects in diodes. That is exceptionally important when electric field strength is maximal and the impact ionization is present in the considered structure.

Based on these considerations, temperature distribution in the diode is found by solving the heat conduction equation:

$$c\frac{\partial T(r,t)}{\partial t} = \nabla \cdot \left[k \nabla T(r,t) \right] + F(r,t) \quad (4)$$

where the thermal conductivity of the material $k(z(x), T(r))$ and the volumetric heat capacity of the lattice c are the functions of temperature and the spatial dependence of the material composition. The intensity of internal heat sources and sinks $F(r,t)$ is determined at the nodes Ω_h from the results of the Monte Carlo simulation in the form:

$$F(x_p, y_p) = \frac{q_L}{e h_x h_y \Delta t} \sum_i w_i W(x_i - x_p, y_i - y_p) \Delta E_i, \quad (5)$$

where the sum is calculated for all simulating particles scattered during the time interval Δt with the absorption (emission) of a phonon or as a result of impact ionization; ΔE_i is the change in the crystal lattice energy due to the scattering of the i charge carrier. The efficiency of heat flow, both at substrate-GaN interfaces and contact metal-semiconductor interfaces, has been described by the thermal boundary conductance (TBC) h_B [15]:

$$q_S = h_B (T_1 - T_2), \quad (6)$$

where q_s is a heat flux across two material interfaces; T_1 and T_2 are temperatures of interface materials. A bottom temperature of the substrate has been fixed at 300 K corresponding to the ideal heat sink. The other boundaries are considered to be adiabatic, and Neumann boundaries condition have been applied for them.

The temperature dependence of material properties is applied as follows. The forbidden gap is

$$E_g(z,T) = z \cdot E_g^{InN}(T) + (1-z) \cdot E_g^{GaN}(T) - b \cdot z \cdot (1-z), \quad (7)$$

where $b = 1.64$ is a bowing parameter [1], $E_g^{InN}(T)$ and $E_g^{GaN}(T)$ are the temperature dependencies of energy gap of InN and GaN correspondently determined by empirical Varshni's formula [1, 18]. The temperature dependence of energy position of higher valleys in

conductor zone is not taken into account. The threshold energy of impact ionization involves (7) as a parameter.

The composition-dependent $In_zGa_{1-z}N$ and temperature-dependent thermal conductivity coefficients $k(z, T)$ are determined by the relation:

$$k\left(z, T(x,y)\right) = \left(\frac{z}{k^{InN}(T)} + \frac{(1-z)}{k^{GaN}(T)} + \frac{z\cdot(1-z)}{b_T} \right)^{-1}, \quad (8)$$

$$\gamma(z) = z\cdot\gamma^{InN} + (1-z)\cdot\gamma^{GaN} . \quad (9)$$

The temperature dependence of the thermal conductivity of binary compounds is determined according to [1, 6]:

$$k(T) = k_0 \left(\frac{T}{300K} \right)^{\gamma}, \quad (10)$$

where b_T = 1.4 W/(m·K) is the bowing parameter [2].

The lattice heat capacity of InGaN is considered to be independent of temperature according to (9). The temperature dependence is accounted for in all scattering probabilities as well [15, 16]. The material parameters used for temperature calculations are given in [1, 2, 6]. To find the solutions for heat equations, the FMG has been applied on grids (1).

3. RESULT AND DISCUDION

The synchronic Monte Carlo method requires calculating the probability of scattering at each moment of simulation, requiring the use of small time intervals. The high scattering being intensive in GaN, the Δt equal to $5\cdot10^{-16}$ s is applied, and the heating time of diode is set up to 13 ns, which is an compromise value to estimate the temperature.

To examine the temperature effect, the simulation has been carried out without taking into account II and self-heating effect. Diodes of the lengths of 1.28 μm, 2.56 μm, and 5.12 μm have been utilized.

The current-voltage characteristics (CVC) of diodes of 1.28 μm and 2.56 μm are shown in Fig. 3.

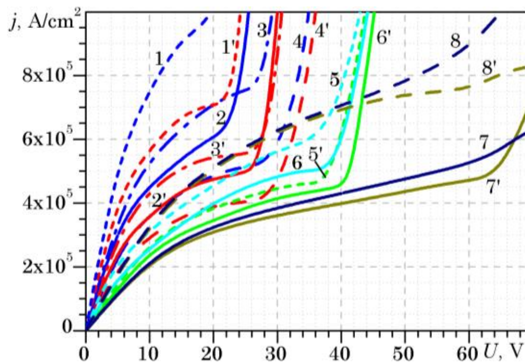

Fig. 3 – Current-voltage characteristics of the diode: 1-8 without self-heating, 1'-8' with self-heating; 1-4, 1'-4' for L_x=0.64 μm, L_y=1.28 μm; 5,5',6,6' for L_x=0.64 μm, L_y=2.56 μm; 7,7',8,8' - L_x=1.28 μm, L_y=5.12 μm; 1,1',3,3',8,8' for N_d=10^{17} cm^{-3}; 2,4-7, 2',4-7' for N_d=6·10^{16} m^{-3}; 1,1',2,2' are type 1, 3-8, 3'-8' are type 2

II is the main factor affecting CVC of diode structures that influences possible modes of operation. It depends strongly on the concentration of carriers. The region of sharp current grooving corresponds to uncontrollable stage of II. The threshold voltage U_p associated with that stage also depends upon diode heating. For the high doping diode (10^{23} m^{-3}) U_p is sufficiently small. For small bias the distribution of electric fields is defined by mesa, and almost identical in diodes of both types, as seen in Fig.4.

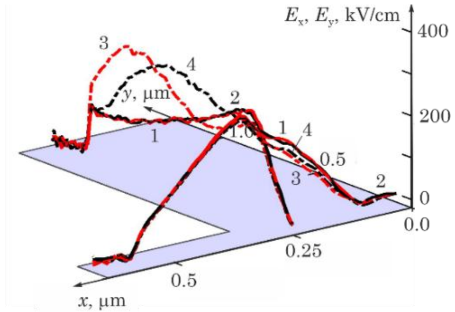

Fig. 4 – Electric field distribution in diodes of 1.28 μm and N_d = 10^{22} m^{-3} with different doping profile: 1, 3 – type 1; 1, 3 – type 2; 1, 2 – 20 V; 3, 4 – 25 V

We can see a forming of unmoving (static) strong electric field domain at the diode cathode simultaneously with the formation of a domain at the anode.

At higher concentration, if bias voltage is close to U_p, maximal electric field in diode type 1 is shifted towards anode. That leads to more intense heating and temperature rise, as seen in Fig. 5.

Maximal temperature in the diode of type 1 is more than 100 K higher than in the diode of type 2, which is crucial for the practical implementation [19].

Using the region with low concentration near meza permits stabilizing electric field and reducing the self- heating effect. Decreasing the doping concentration leads to an even greater reduction, as seen from Fig. 6, c).

The power spectral density (PSD) of output diode current at different bias voltage is shown in Fig. 6. The SPD obtained for diode without self-heating (SH) effect are presented as well. The provided dependencies cover all possible situations.

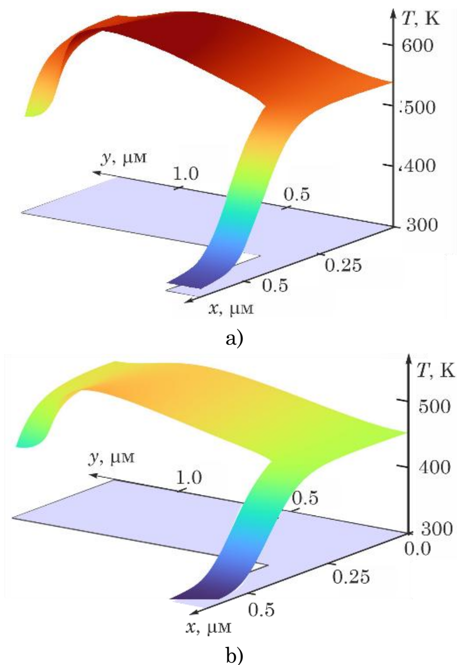

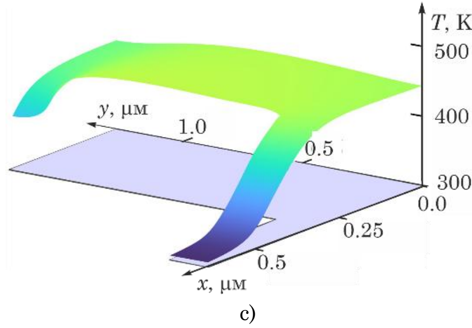

Fig. 5 – Temperature distribution in diodes of 1.28 μm, $U = 25$ V, and different doping profile: a) – type 1; b), c) – type 2; a), b) – $N_d = 10^{17}$ cm^{-3}; c) – $N_d = 6 \cdot 10^{22}$ m^{-3}

With relatively low DC bias, in initial stage of II, the diode can remain stable. Electrons and holes are separated by a strong electric field in CSD. The movement of charge carriers through a diode results in noise at a frequency inverse to the time of movement. In case of the GaN-based diode of the length 1.28 μm, the noise frequencies are expected to be in the range over 200 GHz.

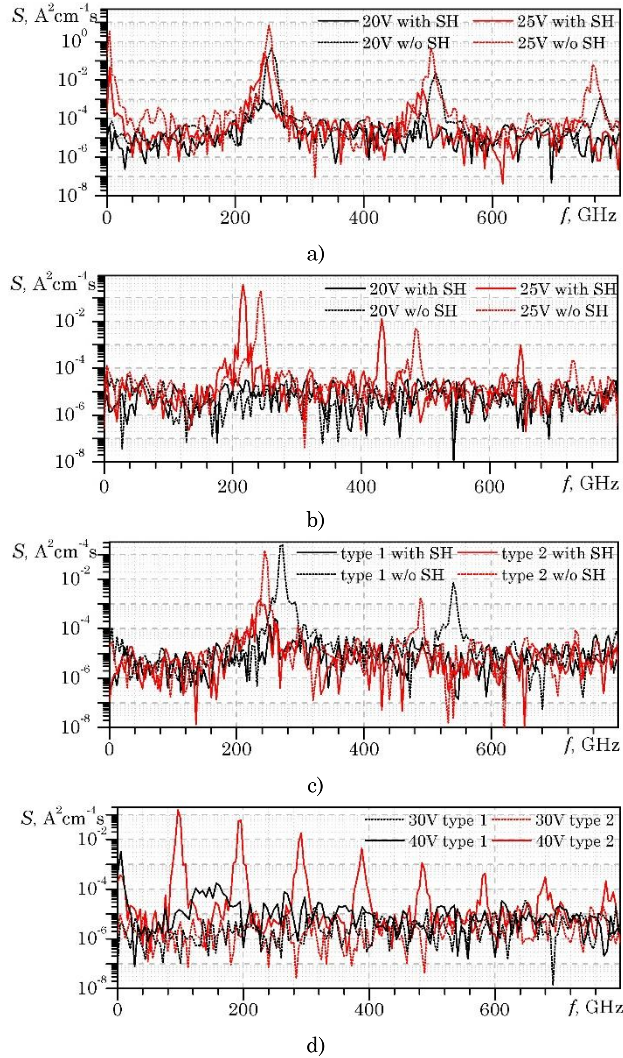

Fig. 6 – PSD for diodes of 1.28 μm (a,b,c) and 2.56 μm (d): a), b) are $N_d = 10^{23}$ m^{-3}; c), d) is $N_d = 6 \cdot 10^{22}$ m^{-3}; a) is type1 b) is type 2

In the diodes of both types, at $T = 300$ K and with a slight change in the bias above U_p, microwave Gunn-like oscillation is observed in the same range, as seen from Fig. 6. However, they almost fully disappear at heating condition for a diode of type 1.

Thus, diode of type 1 can be applied as a source of microwave noise if the electric field magnitude is sufficient for II to appear in the domain. The results obtained for much lower concentrations and longer diodes are shown in Fig. 6 c), d) while ($N_d = 6 \cdot 10^{22}$ m^{-3}) is obtained from the diode simulation while accounting for the self-heating effect. The noise generation in the diode of type 1 and of length 2.56 μm is obtained in a wide frequency band (from about 80 to 200 GHz), Fig. 6(d).

The diode of type 2 can be both the source of a microwave oscillation and noise, at a certain bias range. More general oscillation conditions are not discussed here, but waveform of oscillation can contain many harmonic components, so it is possible to use diode as an active element of a frequency multiplier.

The simulation shows that the diode of length 5.12 μm demonstrates the oscillation at the bias close to the point of corresponding initial stage of II forming a strong electric field domain. The electric field magnitude becomes so high that it leads to uneven heating of the diode even if doping concentration is not large, as seen from Fig. 7.

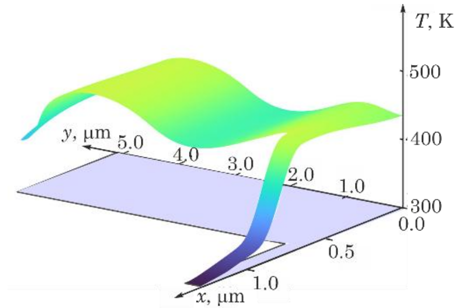

Fig. 7 – Temperature distribution in diodes of 5.12 μm; $L_x = 1.28$ μm, $N_d = 6 \cdot 10^{22}$ m^{-3}; $U = 70$ V; $t_{\text{sim}} = 12.8$ ns

4. CONCLUSIONS

The results of Monte Carlo simulation of self-heating in the GaN diode with graded InGaN mesa have been presented.

It has been shown that proposed diodes are multifunctional active elements, which can be used for different microwave applications. The best prospective use for the diodes is to produce a microwave noise. Diodes with a stabilized cathode domain can have a wide frequency noise band which can be reconfigured by changing the length of the diode channel.

In short-length diode, self-heating is a limiting factor for utilizing a diode as an oscillator. It explains difficulties associated with obtaining a microwave oscillation by the GaN-based device.

A self-heating effect can be reduced by forming in mesa a cathode region with low resistance, as well as controlling the doping concentration. However, it can be difficult to do in domain regime of a diode. Impact ionization occurring in a strong electric field is a factor of heating. That being said, the simulations have shown

that the oscillations appear at a point of initial stage II and it permits to consider II as a factor facilitating appearance of an oscillation.

PSD in a self-oscillation mode contains many high harmonic components of output current, that allows obtaining high frequency oscillation by harmonic extracting. The obtained estimates can be improved by considering longer heating periods, which is the subject for our future investigations.

REFERENCES

1. S. Adachi, *Properties of Semiconductor Alloys: Group-IV, III–V and II–VI Semiconductors* (Wiley: 2009).
2. *III-N Materials, and the State-of-the-Art of Devices and Circuits.* in 3–90 (Berlin: Springer: 2008).
3. C. Gong, M. Mi, Y. Zhou, T. Meng, X. Zhang, T. Liu, X. Jiang, X. Du, F. Chen, X. Ma, Y. Hao, *IEEE Electron Dev. Lett.* **46** No 11, 1950 (2025) https://doi.org/10.1109/LED.2025.3604849.
4. M. Alaei, H. De Pauw, E. Fabris, S. Decoutere, J. Doutreloigne, J. Lauwaert, B. Bakeroot, *IEEE Trans. Electron Dev.* **72** No 9, 4817 (2025) https://doi.org/10.1109/TED.2025.3593216.
5. D. Vasileska, K. Raleva, S. M. Goodnick, *Heating Effects in Nanoscale Devices', in Cutting Edge Nanotechnology* (InTech: 2011).
6. V. Palankovski, R. Quay, *Analysis and Simulation of Heterostructure Devices* (Wien: Springer: 2004).
7. H. Morkoç, *Handbook of Nitride Semiconductors and Devices: Materials Properties, Physics and Growth* (Wiley: 2008).
8. T. Feng, H. Zhou, Z. Cheng, L.S. Larkin, M.R. Neupane, *ACS Appl. Mater. Interfaces* **15** No 25, 29655 (2023) https://doi.org/10.1021/acsami.3c02507.
9. H. Li, R. Hanus, C.A. Polanco, A. Zeidler, G. Koblmüller, Y.K. Koh, L. Lindsay, *Phys. Rev. B* **102** No 1, 014313 (2020) https://doi.org/10.1103/PhysRevB.102.014313.
10. A.S. Hajo, O. Yilmazoglu, A. Dadgar, F. Kuppers, T. Kusserow, *IEEE Access* **8**, 84116 (2020) https://doi.org/10.1109/ACCESS.2020.2991309.
11. D. Vasileska, S. M. Goodnick, G. Klimeck, *Computational Electronics: Semiclassical and Quantum Device Modeling and Simulation* (CRC Press: 2017).
12. K. Nederveen *Ensemble Monte Carlo Simulation of Electron Transport in AlGaAs/GaAs Heterostructures* (Eindhoven: 1989).
13. W. Joppich, S. Mijalković, *Microelectr. J.* **26** No 2-3, xxvii (1995) https://doi.org/10.1016/0026-2692(95)90020-9.
14. O.V. Botsula, V.O. Zozulia, *J. Nano- Electron. Phys.* **12** No 6, 06037 (2020) https://doi.org/10.21272/jnep.12(6).06037.
15. V.O. Zozulia, Y.S. Khodachok, O.V. Botsula, K.H. Prykhodko, *J. Nano- Electron. Phys.* **16** No 6, 06034 (2024) https://doi.org/10.21272/jnep.16(6).06034.
16. O.V. Botsula, K.H. Pryhodko, V.A. Zozulia, *J. Nano- Electron. Phys.* **11** No 1, 01006 (2019) https://doi.org/10.21272/jnep.11(1).01006.
17. C. Jacoboni, L. Reggiani, *Rev. Mod. Phys.* **55** No 3, 645 (1983) https://doi.org/10.1103/RevModPhys.55.645.
18. H. Teisseyre, P. Perlin, T. Suski, I. Grzegory, S. Porowski, J. Jun, A. Pietraszko, T.D. Moustakas, *J. Appl. Phys.* **76** No 4, 2429 (1994) https://doi.org/10.1063/1.357592.
19. J.A. Del Alamo, E.S. Lee, *IEEE Trans. Electron Dev.* **66** No 11, 4578 (2019) https://doi.org/10.1109/TED.2019.2931718.

Ефект саморозігрівання в GaN діоді з варізонною InGaN мезаструктурою

В.О. Зозуля, О.В. Боцула, Л.В. Павлова, О.В. Деговцов

Харківський національний університет імені В.Н. Каразіна, 61077 Харків, Україна

У статті запропоновано багатофункціональні активні елементи, що представляють собою канал на основі n-типу GaN на сапфіровій підкладці з плоскою структурою InGaN (меза) на поверхні каналу. Меза являє собою варізонний шар з молярною часткою Ga, що змінюється зростаючи від 0 на катодному контакті до 1 в каналі, утворюючи складний катод діода. Розглянуто структури з двома типами профілів легування (рівномірне легування та профіль легування з областю низької концентрації) з концентрацією носіїв заряду $6 \cdot 10^{22}$ та 10^{23} м$^{-3}$ у каналі та довжиною 1,28 мкм, 2,56 мкм та 5,12 мкм. Моделювання діода проводилося за допомогою багаточастинкового методу Монте-Карло з урахуванням ударної іонізації та ефекту самонагрівання. Наведено температурну модель, застосовану для аналізу розподілу температури в діоді. Досліджено вплив температури на характеристики діода на постійному струмі та спектральні (шумові) характеристики діодів в умовах сильного електричного поля.

Виявлено, що можливі режими роботи визначаються впливом ударної іонізації, величиною температури та її перерозподілом у каналі діода внаслідок ефекту самонагрівання. Ударна іонізація, що відбувається в сильному електричному полі, призводить до виникнення автоколивань у діоді. Такий режим у діоді з розміром 5,12 мкм демонструє неоднорідний нагрів через виникнення рухомої області сильного поля. Самонагрівання в коротких діодах призводить до збільшення порогової напруги, що відповідає зростанню струму внаслідок ударної іонізації. Було показано, що можна стабілізувати сильне електричне поля поблизу катода використовуючи профіль легування з областю низької концентрації, що сприяє більш однорідному розподілу електричного поля та температурі. Розглянуті діоди можуть бути використані як джерело високочастотного шуму, генератори Ганна або як джерела вищих гармонік у помножувачах частоти.

Ключові слова: Варізонний шар, GaN, InGaN, Діод, Температура, Напруженість електричного поля, Ефект самонагрівання, Ударна іонізація, Шум, Коливання, Густина потужності.